NUCLEAR INSTRUMENTS AND METHODS 126 (1975) 13–23; © NORTH-HOLLAND PUBLISHING CO.

ULTRAVIOLET CHERENKOV LIGHT DETECTOR

P. BAILLON, Y. DÉCLAIS*, M. FERRO-LUZZI, B. FRENCH,
P. JENNI**, J.-M. PERREAU, J. SÉGUINOT* and T. YPSILANTIS

CERN, Geneva, Switzerland

Received 13 February 1975

An increase by a factor ~3.4 in photoelectron emission from Cherenkov light has been observed after coating a standard photomultiplier of the XP1040 class (Philips) with a thin deposit of scintillating material (wavelength shifter). The coating operation is straightforward and requires simple manipulations. We have used coated phototubes in a conventional gas Cherenkov counter exposed to an electron beam at the CERN PS. We measure a figure of merit for the system of $N_0 \sim 170$ photoelectrons per cm.

1. Introduction

The use of Cherenkov counters for particle identification (threshold counters) and velocity determination (differential counters) is a well-established technique in high-energy physics. Current design, performance, and usage has been summarized in a recent review article by Litt and Meunier[1]). In most Cherenkov-counter systems the performance is limited by the number of detected photoelectrons. From the Cherenkov-radiation formula, the number of photons emitted per unit frequency interval is:

$$\frac{\mathrm{d}n_\gamma}{\mathrm{d}\nu} = \frac{2\pi L}{137\,c}\sin^2\theta, \tag{1}$$

where the Cherenkov emission angle is $\theta = \arccos(1/n\beta)$, n is the refractive index of the radiating medium of which the length is L, and β is the particle velocity.

We may then calculate the number of emitted photoelectrons n_e as:

$$n_e = N_0 L \sin^2\theta, \tag{2}$$

with:

$$N_0 = \frac{2\pi}{137}\int_{\lambda_1}^{\lambda_2} \varepsilon_{pc}(\lambda)\,\varepsilon_T(\lambda)\,\varepsilon_R(\lambda)\,\frac{\mathrm{d}\lambda}{\lambda^2}. \tag{3}$$

Hence N_0 represents the specific response of the Cherenkov counter. In eq. (3) $\varepsilon_{pc}(\lambda)$ is the photocathode conversion efficiency, $\varepsilon_T(\lambda)$ is the transmissivity of the radiating medium, and $\varepsilon_R(\lambda)$ is the mirror reflectivity. All Cherenkov counters contain these elements, namely, a detector photocathode, a radiating medium, and usually a reflecting mirror (if no mirror, $\varepsilon_R = 1$). Numerically, the values of N_0 are from 40–60 cm^{-1} for glass-window photomultipliers (PMs) and 80–130 cm^{-1} for quartz-window PMs[1,2]). In actual practice most experiments work with N_0 values between 15 and 60 cm^{-1}, because one or more of the factors in eq. (3) which control N_0 have not been optimised. These low values of N_0 would lead to the design of counters of 10–20 m in length, in order to distinguish a K^+ from a proton at 100 GeV/c. Thus, higher values of N_0 can provide great savings in the Cherenkov counter itself, but also in the size of associated detectors (MWPC or drift chambers), which commonly are placed behind the Cherenkov counter.

In the present work we have attempted to increase N_0 by utilising the uv component of the Cherenkov spectrum. Numerically 3.7 times as many photons are produced between 1050 and 3000 Å (uv region) as are produced between 3000 and 6000 Å (visible region), so if one could utilise the uv photons with the same quantum efficiency as the visible photons, then a gain of 4.7 is possible. The PMs which have LiF windows (and so could be used to detect the uv region directly) have Cs–Te photocathodes, which are 3–4 times less efficient than the bi-alkali or S11 photocathodes which are available in glass- or quartz-window PMs. We have, therefore, chosen to investigate the use of wavelength shifters (WLS) as a possible practical method of utilising the uv component. The use of WLS, such as sodium salicylate, to detect uv radiation is standard practice in uv spectroscopy and space physics[3]). In noble-gas scintillation counters WLS such as tetraphenyl–butadiene (TPB), diphenystilbene (DPS), and many others have been studied and used extensively[4]). The method consists of the deposition of the WLS as a thin film on the glass window of a standard PM. The incident uv radiation is absorbed in the thin film, and

* On leave from IN2P3 (CNRS), France.
** On leave from ETH, Zurich.

causes excited molecular states to be formed, which may subsequently de-excite by the emission of a visible photon which can be detected by the glass-window PM. Since the re-emission is isotropic one might conclude that the total efficiency for this process will be low, hence nullifying the possible gain of 4.7. In addition, these WLS deposits tend to be partially opaque, so that a considerable fraction of the visible component of the Cherenkov radiation is lost. These objections are certainly pertinent; however, the mechanism of photocathode enhancement (see section 4.2) intervenes so that a gain of 3.4 in detected photoelectrons is in fact observed. Results very similar to ours have been reported by Garwin et al.[5]) in a pioneering study of wavelength shifters applied to Cherenkov counters. It is, in fact, surprising that this technique is not more widely known and used in practice. The present investigations confirm their results and attempt to ascertain the mechanism for the gain.

Before embarking on the search for a uv detector it was necessary to ascertain that the other factors (ε_R and ε_T) in eq. (3) did not limit the transmission of the uv component to the detector. Consider first the factor $\varepsilon_R(\lambda)$, which is the reflectivity of the mirror at wavelength λ. Considerable research in the technique of vacuum deposition of Al mirrors with thin MgF_2 or LiF protective layers has demonstrated that essentially 80% and constant reflectivities between 1200 and 2000 Å are possible[6,7]) (see fig. 1). Above 2000 Å the reflectivity rises slowly to a value of 90% in the visible. The preparation of such mirrors requires fast ($\sim$1 s) deposition of the Al mirror on an unheated substrate in a very good vacuum ($\sim 10^{-7}$ torr), followed immediately by the deposition of the protective layer of

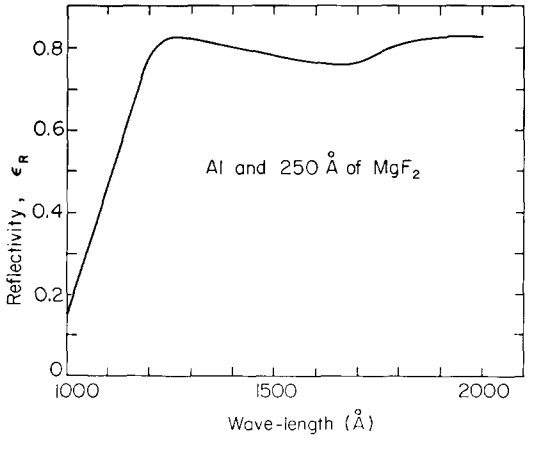

Fig. 1. Reflectivity at normal incidence of an Al mirror coated with 250 Å MgF_2 versus wavelength.

250 Å of MgF_2. Mirrors not so prepared will generally have very bad reflecting properties in the uv. It has been observed that such mirrors are stable in air, losing only 2% reflectivity after one year. The MgF_2 layer is necessary to protect the Al mirror from oxidation, and since MgF_2 is transparent down to 1150 Å it is clear why the reflectivity of the MgF_2-overcoated Al mirrors falls below 1200 Å. Since very few Cherenkov-radiating gases (only He and Ne) are transparent below 1200 Å, the fall in reflectivity does not represent a serious limitation.

The factor $\varepsilon_T(\lambda)$ is the radiating-gas transparency. Absorption coefficients for various gases are available in the literature[8]); however, it is sufficient to note that most of the lowest-refractive-index gases (which are needed as Cherenkov radiators for very high energies) are transparent down to or near 1200 Å. He, Ne, H_2, Ar, N_2 and Kr are largely transparent and should give high values of N_0, if all other factors in eq. (3) are optimised.

2. Measurements with a lithium-fluoride radiator

2.1. The setup

In order to avoid introducing (initially) unknown or poorly known absorption and reflectivity corrections into the measurement of N_0, we have constructed the apparatus shown in fig. 2. It consists of a 5 mm thick lithium fluoride (LiF) crystal and an 11 cm diameter PM, all contained in an iron cylinder which could be evacuated to 5×10^{-2} torr. Since LiF is transparent down to 1050 Å, a fast particle (2 GeV/c π^-) passing through the crystal will produce a characteristic $1/\lambda^2$ Cherenkov spectrum, cut off at 1050 Å. By orienting the crystal at 45° to the beam (the average Cherenkov angle in LiF), a fraction of the emitted Cherenkov cone enters the PM window normally. With this configuration, the fast particle does not pass through the PM window, where it would produce Cherenkov radiation which would obscure the effect under study. A simple geometrical-optics calculation allows one to determine the distributions of Cherenkov light at the plane of the PM window (see fig. 2a). This calculation includes the variation of the LiF refractive index with wavelength[9]) (see fig. 3b), the transparency of the LiF crystal[10]) (see fig. 3a), and refraction at the crystal–vacuum interface. The differential acceptance onto the 11 cm diameter PM is shown in fig. 4. Even though the acceptance falls rapidly at short wavelengths, the absolute number of photons in the far uv is large as is shown in fig. 5, which shows the number of photons hitting the PM versus wavelength. The peak of the

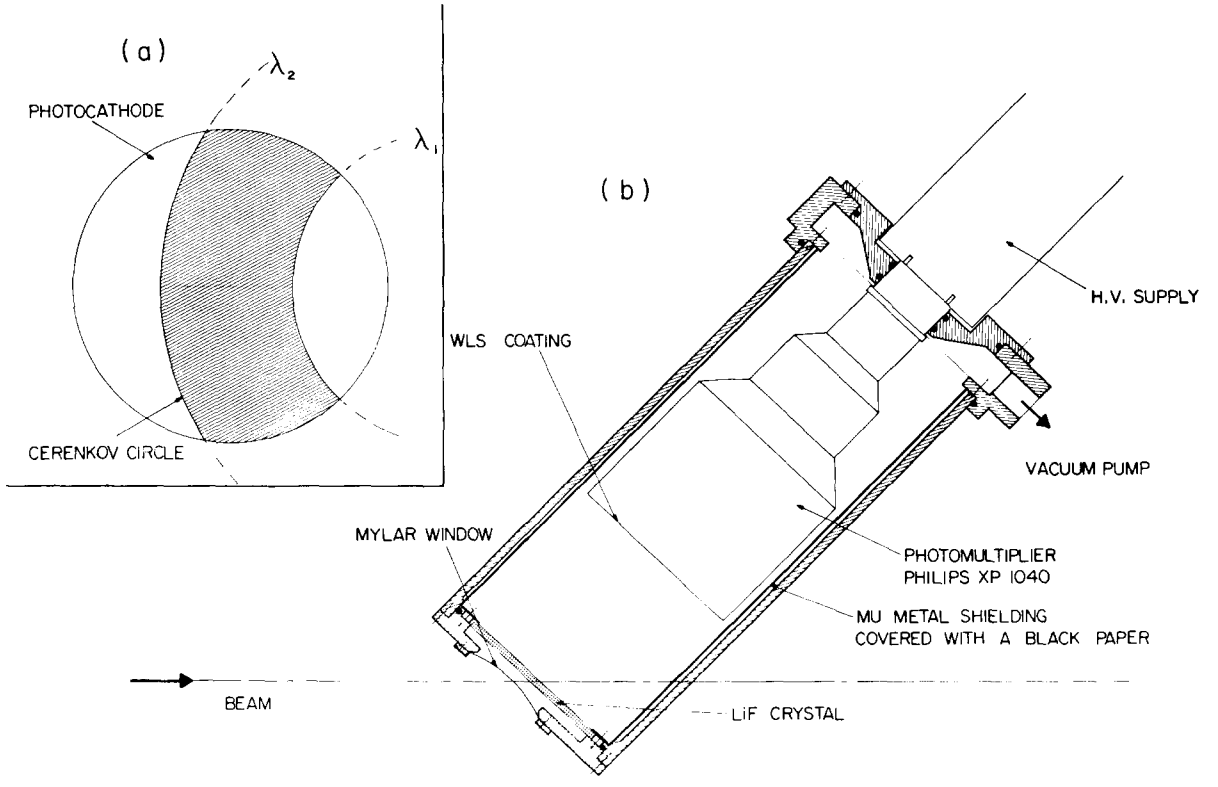

Fig. 2. (a) Distribution of Cherenkov light at the photomultiplier window. (b) Apparatus containing LiF crystal and photomultiplier.

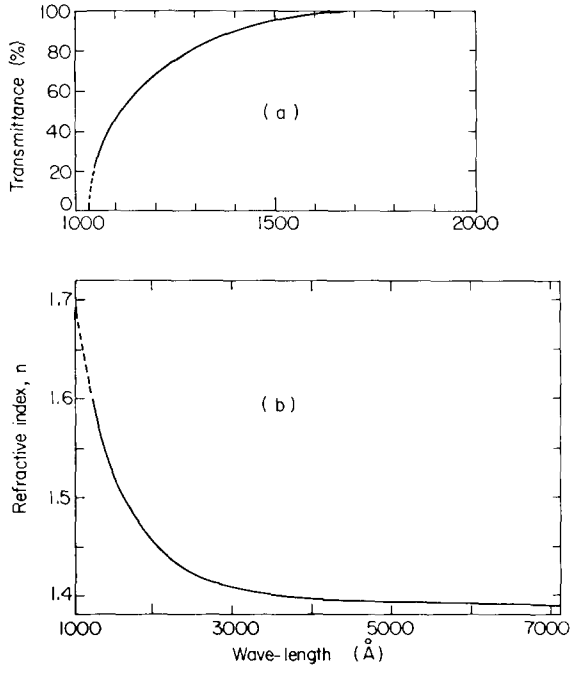

Fig. 3. (a) Transparency of a 1.9 mm thick LiF crystal versus wavelength. (b) Refractive index of LiF versus wavelength.

distribution is at 1350 Å, with a still large contribution even at 1050 Å. This setup was used as a standard source of uv photons, and resulted in (190 ± 14) photons hitting the PM for each incident π. The number of photons in the uv region is 145 and the number in the visible is 45, so the ratio of total to visible photons is 4.2.

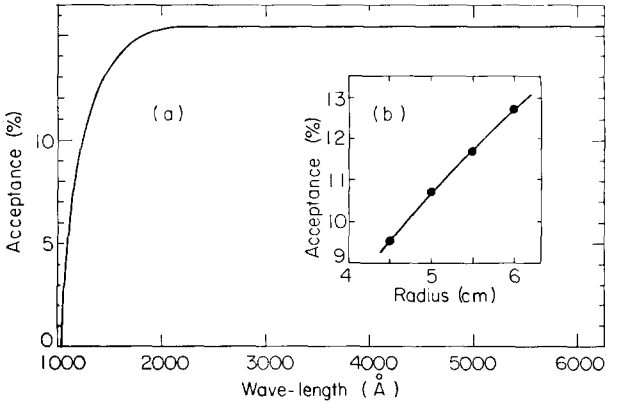

Fig. 4. Differential acceptance of Cherenkov radiation from the LiF crystal onto an 11 cm diameter photomultiplier. Inset: total acceptance between 1000 Å and 6000 Å versus effective PM radius.

The complete experimental setup is shown in fig. 6. The beam momentum was 2 GeV/c negative, and consisted mainly of π's with perhaps 5–10% of $K^- + \bar{p}$ (the Q12 beam of the CERN PS). The trigger requirement was $S_1 S_2 S_3 S_4 \bar{C}_1$, which rejected electrons (C_1 at 1 atm. of air). Here the particular particle selected was not critical, since the LiF index is so high that all 2 GeV/c particles give Cherenkov radiation at 45°. The scintillators S_3 (5 mm ∅) and S_4 (10 mm ∅) were small, and defined the radiating region of the crystal to be at the intersection of the PM axis with the crystal plane. The signal from the PM was passed through an attenuator, a linear gate (gate generated by the $S_1 S_2 S_3 S_4 \bar{C}_1$ coincidence), a charge amplifier, and hence into a digital pulse-height analyser. The background noise and drift was subtracted digitally by opening a delayed gate (uncorrelated with an incident particle) 0.7 ms after the trigger signal. We have verified that the pulse-height response is linear to ±1% with the input pulse over the range of the pulse-height analyser. Typically, the beam intensity was reduced so as to have a few thousand pions per machine burst of ~350 ms. A measurement of 20 000 counts was obtained in about 5 or 10 min. During data taking the pulse-height spectra could be displayed on a Tektronix 611 display unit. The final spectra were printed out and also read out on magnetic tape for subsequent analysis.

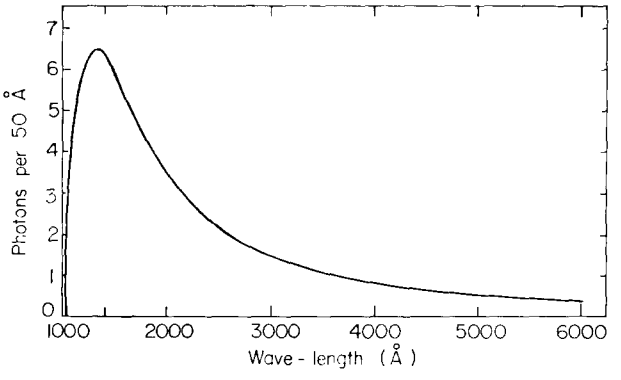

Fig. 5. Number of photons per 50 Å interval hitting the PM versus wavelength.

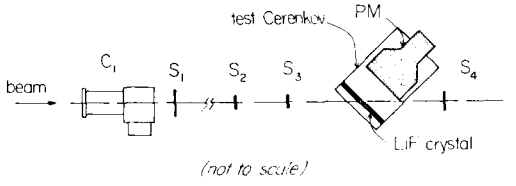

Fig. 6. Experimental setup with LiF crystal.

2.2. Deposition of wavelength shifters on PM window

We have generally used the method of vacuum evaporation of the organic wavelength shifter directly

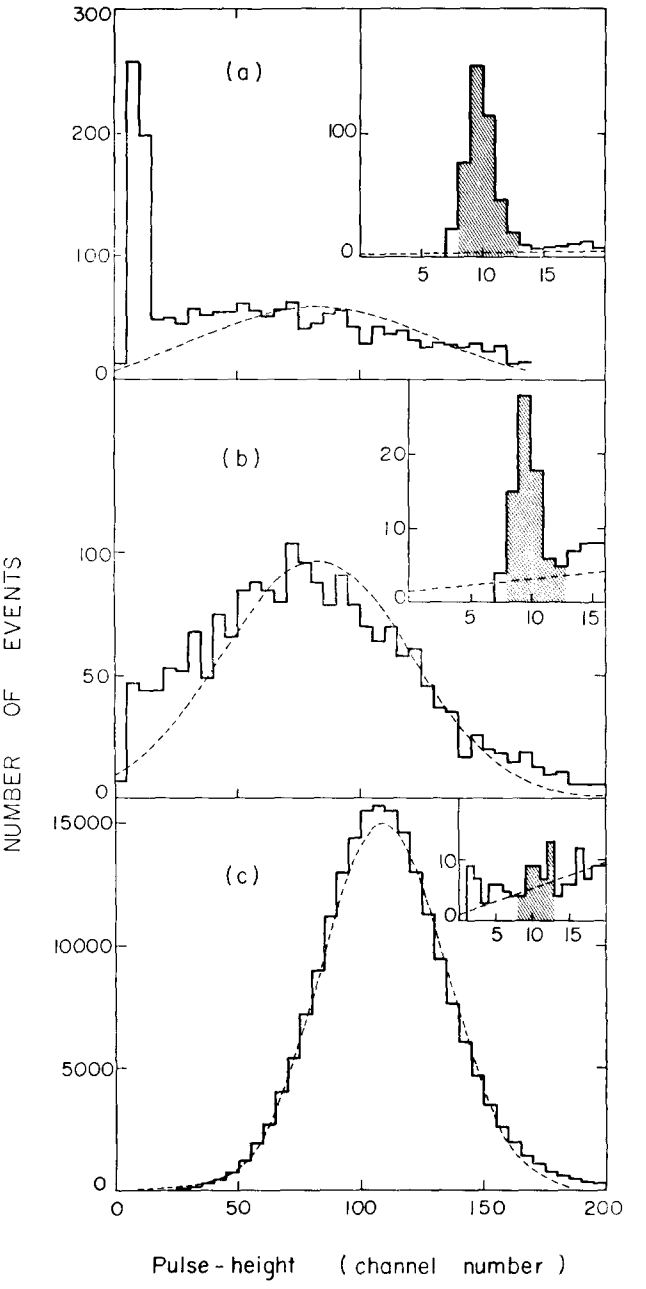

Fig. 7. Representative pulse-height spectra: Insets show the zero pulse-height region in detail (zero pulse height is channel 10). Shaded areas indicate the region of zero efficiency. Dotted curves are the Gaussians calculated from first and second moments of the distribution. (a) Large inefficiency, (b) medium inefficiency, and (c) small inefficiency.

onto the PM window. The WLS was weighed in a Mo boat, and the PM was enclosed with it in a vacuum vessel and pumped until a pressure of 2 to 4×10^{-5} torr was achieved. The distance between the boat and the PM face was about 12 cm (limited by the size of the vacuum vessel). A somewhat larger distance would probably be desirable, since some of the deposits were noticeably more transparent at the PM rim. The rate of evaporation was not strictly controlled. The most uniform deposits were obtained by slowly raising the temperature of the sample until the WLS liquified and then allowing deposition to occur without any subsequent increase in temperature. The thickness of the deposits was monitored by an oscillating quartz crystal placed at about 25 cm from the sample. In some cases the WLS could not be vacuum evaporated because it decomposed at high temperatures. In such cases we deposited the WLS by evaporating a solution of WLS in methyl alcohol on the PM face. The only case where this method gave significant gains was with sodium salicylate (SS); however, this gain was significantly smaller than the best vacuum-evaporated WLS.

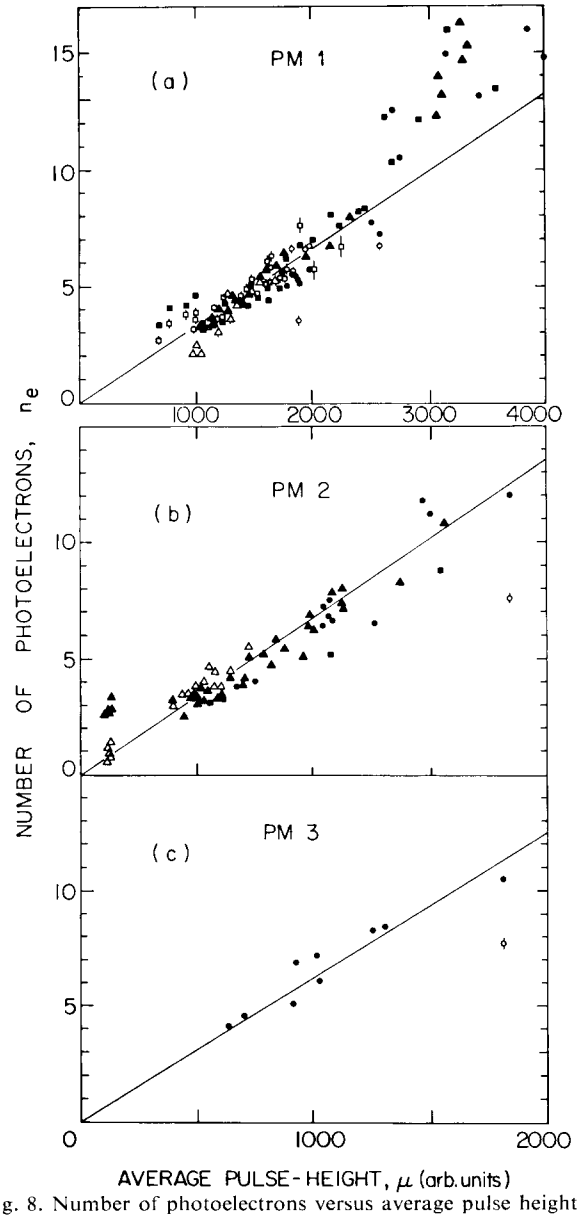

Fig. 8. Number of photoelectrons versus average pulse height μ for three different photomultipliers used in this experiment. Open points are from inefficiencies, closed points are from μ^2/σ^2 measurements. Circles and squares correspond to the lithium fluoride set up and triangles to the gas Cherenkov set up.

2.3. The analysis of the pulse-height spectra

The spectra recorded during our runs can be roughly classified into three categories. Fig. 7 shows an example of each. The peak near the 10th channel in figs. 7(a) and (b) represents the number of triggers with zero response from the PM. We can use the latter to define the photocathode inefficiency ϕ as the ratio of zero response to total triggers. One can use ϕ to calculate the average number n_e of emitted photoelectrons by recalling Poisson's law:

$$\phi = \exp(-n_e). \tag{4}$$

For finite statistics the value of n_e derived from eq. (4) is meaningful only if ϕ is sufficiently large. In practice this means that n_e must be smaller than ~ 5 to provide a significant determination of ϕ. For larger values of n_e the spectrum is practically indistinguishable from that of a Gaussian: see fig. 7(c), for example. In this case the average pulse height μ and the rms width σ are proportional to n_e and $\sqrt{n_e}$ respectively (the proportionality constant is the gain of the PM). From this it follows that the ratio μ^2/σ^2 gives directly the value of n_e (independent of the PM gain). For intermediate values of n_e, before the distribution becomes strictly Gaussian, we encounter cases like the one illustrated in fig. 7(b). Here the Gaussian interpretation of μ^2/σ^2 and the measurement of ϕ are both marginally valid. This provides a useful consistency check between the two determinations of n_e.

In essence, each spectrum yields one or two possible values of n_e according to whether μ^2/σ^2, or ϕ, or both can be correctly interpreted. All these values have been plotted as a function of μ – whenever the latter was meaningful, i.e., for the spectra of the type shown by figs. 7(b) and 7(c). An example of these plots is shown in fig. 8 for each specific PM. The agreement of the ϕ and the μ^2/σ^2 determination of n_e, and a linear dependence on μ is quite good for n_e smaller than ~ 8

TABLE 1

Response of wavelength shifters.

WLS[a]	thickness (μg/cm^2)	n_e	N_0 (cm^{-1})	N_0(air)/N_0	$G=N_0/N_0'$
PM no. 1; $n_e'=3.7$, $N_0'=69$ cm^{-1}.					
PT	200	13.3	275	–	3.99
PT	40	12.8	266	0.64	3.86
TPB	220	11.9	246	0.60	3.56
TPB	74	11.0	229	0.65	3.31
TPB	25	10.7	222	0.68	3.22
PQ	10	9.0	186	0.73	2.70
SS	unknown	8.6	178	–	2.57
Fluorene	12	6.6	136	–	1.97
TS	18	6.5	134	–	1.94
PPO	unknown	6.2	129	–	1.87
Pyrene	80	5.9	123	–	1.78
PM no. 2; $n_e'=3.7$, $N_0'=69$ cm^{-1}.					
PT	10	12.8	265	0.60	3.84
PT	220	11.5	238	0.59	3.45
PT	90	10.5	218	0.65	3.16
PT	80	10.2	211	0.64	3.06
PT	160	10.1	209	0.63	3.03
PT	20	9.5	197	0.64	2.86
PT	7	7.2	150	–	2.18
SS	unknown	7.4	152	–	2.21
PQ	5	7.1	147	–	2.13
DPB	80	5.5	114	–	1.65
Coronene	130	5.1	106	0.81	1.54
Cadmium propionate	unknown	4.6	95	–	1.37
POPOP	10	4.2	86	–	1.25
ANPO	90	3.8	79	–	1.14
Fluorescein	unknown	3.1	65	–	0.94
PM no. 3; $n_e'=2.8$, $N_0'=53$ cm^{-1}.					
TPB	60	11.4	236	–	4.45
TPB	120	8.4	173	0.61	3.26
TPB	160	6.4	132	–	2.49
PT	unknown	7.9	164	–	3.09
PT	unknown	6.4	132	–	2.49
PT	4	4.7	98	–	1.85
PQ	40	6.4	132	–	2.49
DPS	10	5.8	120	0.62	2.26
SS	unknown	4.4	92	–	1.74

[a] We have abbreviated the names of the wavelength shifters. TPB = tetraphenylbutadiene, PT = p-terphenyl, PQ = p-quaterphenyl, DPS = diphenylstilbene, SS = sodium salicylate, TS = trans stilbene, PPO = diphenyloxazole, DPB = diphenylbutadiene, POPOP = phenylene phenyloxazole, ANPO = alpha naphthyl phenyloxazole.

(notice that the majority of our measurements are in this range). For n_e larger than 8 the curve of μ^2/σ^2 vs μ for PM no. 1 is no longer linear [fig. 8(a)]. This happens because of the saturation of the PM gain as n_e becomes large, and causes the value of μ and σ to be underestimated. We have systematically used the straight line through the origin (shown in fig. 8) to convert μ into n_e for this particular PM. For large values of n_e, this tends to underestimate n_e and gives us conservative values for N_0. Whenever μ was not reliable (as is frequently the case for $n_e<2$), we have directly used ϕ. Our results for different WLS are listed separately in table 1 for each of three different PMs (Philips XP1040, 11 cm diameter, glass window) used in these measurements. The value n_e' is the measured number of photoelectrons for the uncoated tube, and N_0' is the corresponding value of N_0, calculated by using the acceptance calculations in fig. 4. We list in many cases the ratio of N_0(air)/N_0, where N_0 is the value measured in vacuum and N_0(air) the value with air between crystal and PM. In calculating N_0, N_0', and N_0(air) we use the following formula:

$$N_0 = n_e \Big/ \left[AL\left(1-\frac{1}{n^2}\right)\right], \tag{5}$$

with A the acceptance over the wavelength interval (from fig. 5), L the effective length of the radiator (0.5 cm/cos 45°), and n the index of refraction at the average of the photon distribution in the interval

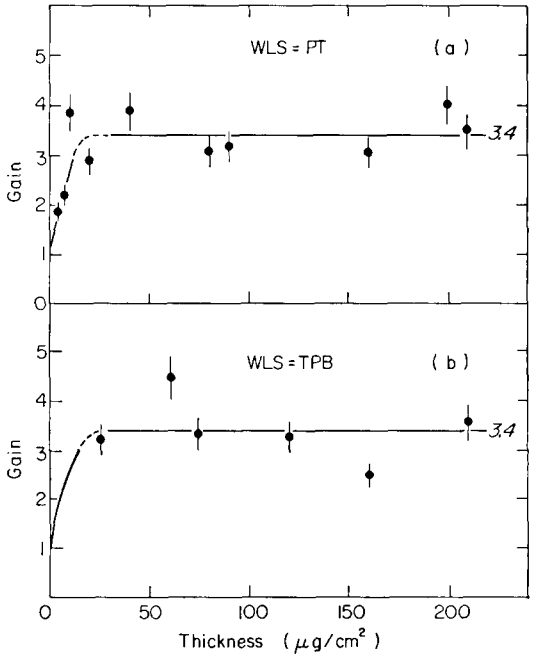

Fig. 9. (a) Gain versus thickness for wavelength shifter p-terphenyl; (b) gain versus thickness for wavelength shifter tetraphenylbutadiene.

[from fig. 3(a) and fig. 5]. The relevant interval for N_0 is from 1050 to 6000 Å, for N_0(air) from 1700 to 6000 Å, and for N_0' from 3000 to 6000 Å.

It can be seen from table 1 that quite substantial gains ($G = N_0/N_0'$) are obtained with PT (p-terphenyl), and with TPB (tetraphenylbutadiene) ($G \sim 3.4$), followed by PQ (p-quaterphenyl) and SS (sodium salicylate) ($G \sim 2.5$). Only in the cases of PT and TPB were enough different thicknesses tried to obtain the gain-versus-thickness dependence. These are shown in figs. 9(a) and (b). The curves are visual fits and show that the exact thickness is not critical. We conclude that the gains with either TPB or PT are similar and about 3.4 in magnitude. It will be noted that for the best wavelength shifters N_0(air)/N_0 is between 0.6 and 0.65. Since oxygen has a large absorption of the uv between 1700 and 1200 Å [8]), one expects this effect. In fact, from the spectrum of fig. 5, we find about 35% of the photons from our source lie in this range. This clearly demonstrates the high uv sensitivity of the detector.

The life-times of the excited states in PT and TPB are 5.5 and 4.0 ns, respectively[4]), so that no important time delay is introduced by using these WLS. The spectrum of re-emission in both cases is relatively sharp (±200 Å) and centred near 4200 Å, which is about the peak response of the PM.

3. Gas Cherenkov radiators

3.1. The setup

After ascertaining the best wavelength shifters with the LiF setup, we installed the apparatus, shown in fig. 10, in the beam. It consists of a 2.5 m long tube, 18 cm in diameter, with a flat reflecting mirror* oriented at 45° to the beam, and a PM detector. The whole system could be pumped to a pressure of about 10^{-1} torr before filling with the gas under measurement. A special feature of this counter was a movable black screen (15 cm diam.), which was remotely positionable so as to allow variation in the length L

* This mirror was made by J. Haidenhain Optik of Traunreut/Obb, West Germany, according to the method described in section 1. They claim 80% reflectivity down to 1200 Å, and our measurements support this claim.

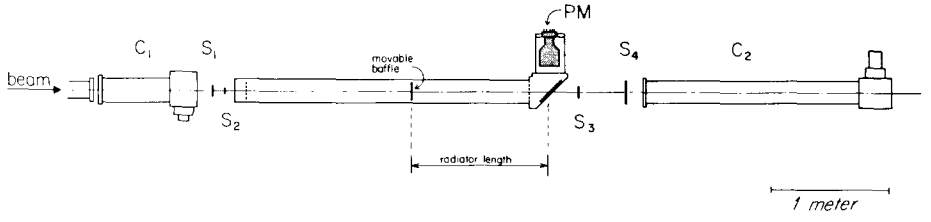

(a)

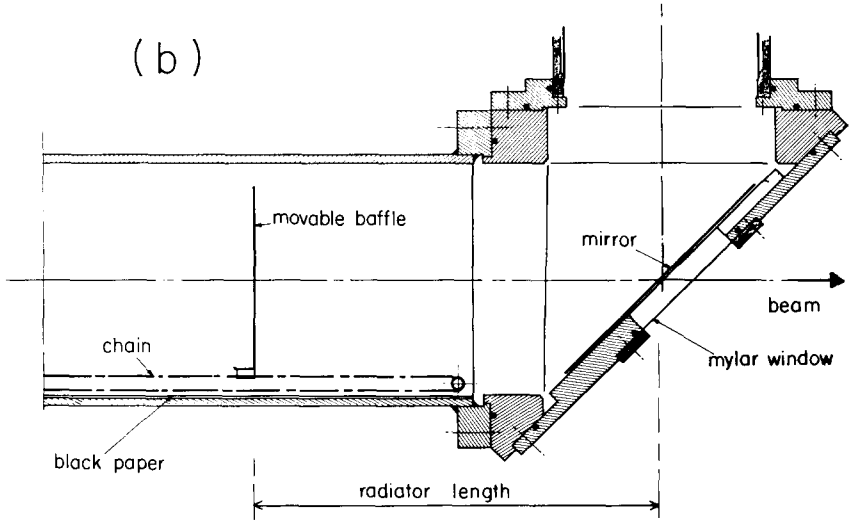

Fig. 10. (a) Gas Cherenkov counter setup. (b) Details of screen and mirror assembly.

of the gas radiator. In this configuration we used 2 GeV/c e^- as the primary particles. The trigger coincidence was $C_1S_1S_2S_3S_4C_2$, with C_1 and C_2 standard one-atmosphere-air Cherenkov counters. It was necessary to define the electrons twice (with C_1 and C_2), because a π meson of the beam produces delta rays (with low probability) which cause C_1 or C_2 to count. The probability that the same π causes C_1 and C_2 to count is negligible. From eq. (2) we note that n_e must be linear in L, and the slope of the curve determines

$$N_0 \sin^2\theta = N_0\left(1 - \frac{1}{n^2}\right).$$

3.2. Results

The measurements were performed using different gases together with coated and uncoated PMs. We have restricted the choice of WLS to the two best ones (see section 2.3), namely PT and TPB.

Fig. 11 shows the plots of n_e' as a function of L for the uncoated PMs and various gases. The linear dependence on L is evident up to the values of L for which the Cherenkov cone is not fully accepted by the PM (e.g. for freon 12 and 13). In fig. 12 are the corresponding plots for coated PMs and various gases. The values of N_0 determined from the slopes of these curves and the gas refractive indices are shown in fig. 13.

It is seen from fig. 13 for the uncoated PMs and the most transparent gases (Ar, CO_2, N_2 are highly transparent in the visible) that $N_0' = 57$, which, when corrected for mirror reflectivity of 90% in the visible, gives $N_0' = 63$. This agrees reasonably well with the value of 69 found in the LiF measurements for PM no. 1 and PM no. 2 (these are the only PMs used in the gas-counter measurements). For N_2 and a TPB-coated PM we find $N_0 = 174$, which, with correction for mirror reflectivity (80% in the uv), gives $N_0 = 218$. Thus the gain (referred to the no-mirror LiF setup) is $218/63 = 3.45$, which agrees completely with the results of section 2.3. It is, however, more appropriate to consider the gain with the mirror as $174/57 = 3.05$. This is the highest value we have observed in this

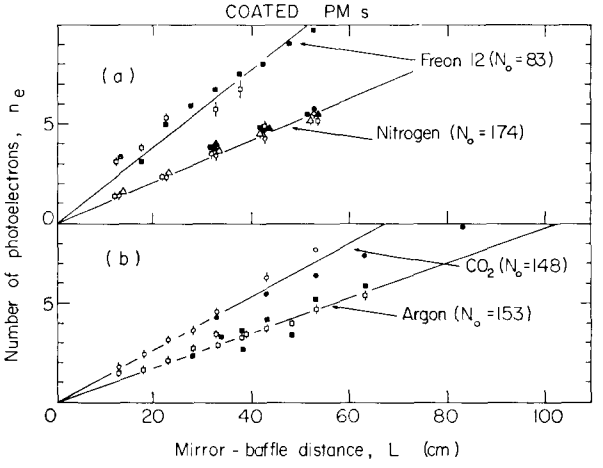

Fig. 12. Number of photoelectrons n_e versus gas length for photomultiplier no. 1, coated with 220 μg/cm^2 of TPB and various gases. Open points are from inefficiencies, closed points are from μ^2/σ^2 measurements.

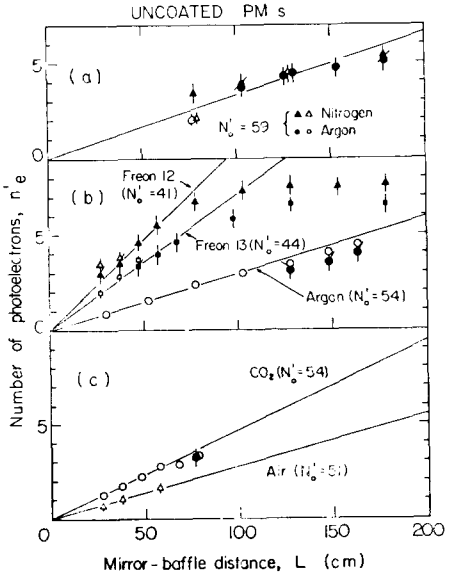

Fig. 11. Number of photoelectrons n_e' versus gas length L for uncoated photomultipliers and various gases. Open points are from inefficiencies, closed points are from μ^2/σ^2 measurements.

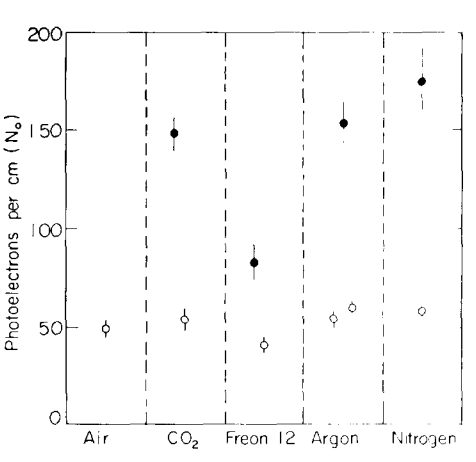

Fig. 13. Summary of values of N_0 measured for various gases with (closed points) and without (open points) wavelength shifter (220 μg/cm^2 TPB).

TABLE 2
Quantum efficiencies of photomultipliers.

PM	Diameter (cm)	Measured ε_m	Rated ε_R	$F=\varepsilon_m/\varepsilon_R$
Philips XP 1040	11	0.128	0.213	0.60
RCA 8454 (Quantacon)	11	0.130	0.295	0.44
Philips 56DUVP	5	0.147	0.229	0.64

configuration. The gain in argon was 2.6, in CO_2 2.7, and in freon-12 2.0.

With this setup we have also measured the response of an RCA 8454 PM (Quantacon, 11 cm diam. bialkali photocathode, borosilicate window with 2500 Å cut-off) with N_2 as the radiating gas. We find $N_0' = 120\ \mathrm{cm}^{-1}$ for the uncoated PM, and $N_0 = 160\ \mathrm{cm}^{-1}$ with 130 μg/cm^2 of TPB coating. The value $N_0' = 120$ for the uncoated quantacon is much lower than expected for a PM whose quantum efficiency is rated at about 28% (see section 4.1). In addition, a gain of only 1.3 is obtained with the TPB coating, which seems to indicate that for some unknown reason the gain mechanism (see section 4.2) is much less efficient for this photocathode. The PM was operated, as recommended by RCA for maximum quantum efficiency, with 670 V between the photocathode and the first dynode.

4. Quantum efficiency and photocathode enhancement

4.1. Quantum-efficiency measurements

From section 3 we found $N_0' = 63\ \mathrm{cm}^{-1}$ corrected for mirror reflectivity. This may be compared to the value obtained (for the same PM) in the LiF radiator setup of $N_0' = 69\ \mathrm{cm}^{-1}$, so the measurements agree and we take $N_0' = 66\ \mathrm{cm}^{-1}$ as the average. From eq. (3) we have (for $\varepsilon_R = \varepsilon_T = 1$):

$$N_0 = \frac{2\pi}{137}\int_{\lambda_1}^{\lambda_2} \varepsilon_{pc}(\lambda)\,\frac{d\lambda}{\lambda^2}.$$

We determine the relative spectral response of a S11 photocathode (XP1040) from the Philips Electron Tube Data Handbook. Integrating between the limits of sensitivity (2900–6600 Å) we obtain:

$$N_0' = 516\,\varepsilon_m,$$

where ε_m is the maximum quantum efficiency (in this case at 4200 Å); thus for $N_0' = 66\ \mathrm{cm}^{-1}$ we get $\varepsilon_m = 0.128$. This tube was evaluated by Philips to have a radiant cathode sensitivity of 75 mA/W at 4370 Å, which corresponds to a rated quantum efficiency of $\varepsilon_R = 0.213$. Since the manufacturers' method of measurement of quantum efficiency does not include the efficiency of collection of photoelectrons from photocathode to the first dynode, we conclude that the collection efficiency is $F = \varepsilon_m/\varepsilon_R = 0.6$ for this PM. Similar results have been reported[11]) for diverse PMs where the measured quantum efficiency is between 2 to 3 times lower than the rated value.

We have made measurements on three different PMs and our results are summarised in table 2. We conclude that for practical use one must take about 50% of the manufacturer's rated value as the actual quantum efficiency.

4.2. Photocathode enhancement and wavelength shifters

It has been observed by Gunter et al.[12]), and independently by Rambo[13]) that, if light is introduced (with a prism) into the photocathode window at an angle greater than the critical angle θ_c ($n\sin\theta_c = 1$), then total internal reflection will occur and the photon will pass through the photocathode layer many times, hence enhancing the probability of conversion to an electron. This is shown schematically in fig. 14(a). Gains of 2 to 3 in quantum efficiency at 4000 Å have been obtained[14]). We are not advocating the use of such prisms to introduce the light into the photocathode, because angle and surface area restrictions are severe; however, in some particular cases, where small images and divergences occur, this might be useful. We believe,

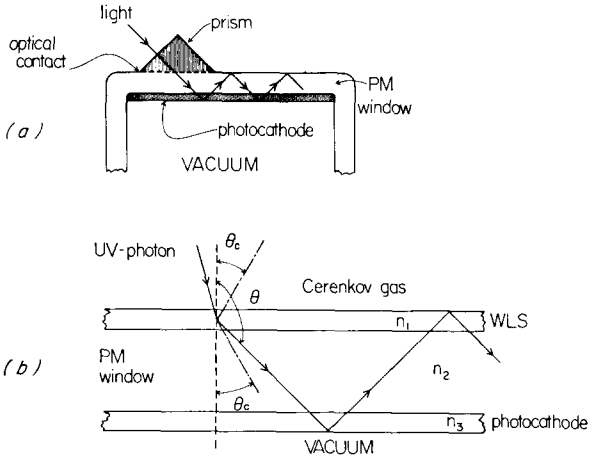

Fig. 14. (a) Schematic diagram to illustrate the principle of photocathode enhancement. (b) Photocathode enhancement for photons emitted by the wavelength shifter.

instead, that this mechanism explains the large gains we have obtained using wavelength shifters. From fig. 14(b) one may see that the WLS (refractive index n_1), the PM window (n_2), and the photocathode (n_3) are all in optical contact and comprise a layered optical medium. If an incident uv photon is absorbed at a point inside the WLS and is re-emitted at an angle θ_1 relative to the normal, then:

$$n_1 \sin\theta_1 = n_2 \sin\theta_2 = n_3 \sin\theta_3 = k = \text{constant}, \tag{6}$$

so that light in the layered medium will be totally reflected whenever it encounters a layer of index $\eta < k$. Since for almost all WLS material $n_1 < 1.5$, PM-glass $n_2 = 1.5$, and for all photocathodes $n_3 \sim 3$, it follows that total internal reflection will occur at WLS–gas interface, or at the photocathode–vacuum interface. Thus the WLS introduces about 60% of the re-emitted light into the PM glass window at angles greater than the critical angle. Consider a single re-emitted photon at angle θ with respect to the upward normal. If $\theta < \theta_c$ (zone 1) the photon will escape upward, if $\theta_c < \theta < \pi - \theta_c$ (zone 2), the photon internally reflects at top and bottom surfaces, if $\pi - \theta_c < \theta < \pi$ (zone 3), then the photon passes once through the photocathode layer normally. The fractional solid angles f_i for emission into zone i are $\frac{1}{2}(1-\cos\theta_c)$, $\cos\theta_c$, $\frac{1}{2}(1-\cos\theta_c)$, for $i = 1, 2, 3$, respectively. Hence the effective quantum efficiency ε' for a photon re-emitted (at wavelength λ) by the WLS is:

$$\varepsilon' = \varepsilon_1 f_1 + \varepsilon_2 f_2 + \varepsilon_3 f_3 . \tag{7}$$

Clearly $\varepsilon_1 = 0$ (since this photon escapes upward), $\varepsilon_3 = \varepsilon_{pc}(\lambda) \equiv \varepsilon$ since it passes only once through the photocathode, and:

$$\varepsilon_2 = \varepsilon(1 + e^{-\mu t} + e^{-2\mu t} + e^{-3\mu t} + \ldots) = \frac{\varepsilon}{1 - e^{-\mu t}}, \tag{8}$$

where μ is the photoelectric absorption coefficient for the photocathode layer of thickness t. The first two terms in eq. (8) correspond to the first bounce, the next two to the second bounce, etc. The photocathode quantum efficiency ε is related to $e^{-\mu t}$ by:

$$\varepsilon = \tfrac{1}{2}(1 - e^{-\mu t})\, p, \tag{9}$$

where the factor two occurs because only half of the produced photoelectrons are emitted on the vacuum interface, and p is an unknown extraction probability. Thus we find for many bounces [from eqs. (8) and (9)]:

$$\varepsilon_2 = p/2.$$

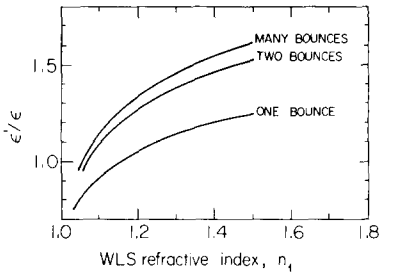

Fig. 15. The quantum efficiency ε' for re-emitted photons for one, two, and many bounces versus the index of refraction n_1 of the wavelength shifter. ε is the quantum efficiency of the photomultiplier at frequency λ of the re-emitted photon.

Gunter et al.[14]) find $\varepsilon_2 = 0.4$ for many bounces with $\varepsilon = 0.2$ (photocathode enhancement of 2 at 4000 Å), so $p = 0.8$.

We can now calculate ε_2 for one bounce:

$$\varepsilon_2(1) = 2\varepsilon(1 - \varepsilon/p); \tag{11}$$

hence:

$$\varepsilon'/\varepsilon = \tfrac{1}{2}(1 - \cos\theta_c) + 2(1 - \varepsilon/p)\cos\theta_c . \tag{12}$$

This ratio ε'/ε is shown in fig. 15 for one, two and many bounces for different values of WLS refractive index n_1. We note that, even for the one-bounce case and $n_1 = 1.25$, $\varepsilon'/\varepsilon = 1.1$, which means that each re-emitted photon is counted by the PM with an efficiency ε' at least equal to ε (the efficiency for visible photons), even with solid angle losses due to isotropic re-emission.

We can now try to estimate the absolute efficiency η of the wavelength shifter for capture of a uv photon and re-emission in the visible as:

$$\eta = \frac{3.4}{(4.2) \times (1.1)} = 0.74, \tag{13}$$

where 3.4 is the average gain with the WLS (see section 2.3), 4.2 is the ratio of uv to visible photons (see section 2.1) and 1.1 is the quantum-efficiency ratio just calculated. The best value of η for SS is given as 0.6–0.65[3]), and Brunet et al.[15]) find TPB or PT are between 20–60% more efficient than SS. So the expected value of η is between 0.7 and 1.0, which is not in disagreement with our result.

We wish to thank Mr P. Queru, Mr J. Perez, Mr B. Goret and their colleagues in the Design Group at CERN-TC for their efforts in designing the equipment. Special thanks go to Mr C. Detraz for his work throughout the experiment.

References

1) J. Litt and R. Meunier, Ann. Rev. Nucl. Sci. **23** (1973).

2) D. D. Yovanovitch, D. R. Rust, J. Ambats, R. A. Lundy, S. M. Pruss and C. W. Akerlof, Nucl. Instr. and Meth. **94** (1971) 477.

3) J. A. R. Samson, *Techniques of vacuum u.v. spectroscopy* (J. Wiley, New York, 1967) p. 216.

4) J. B. Birks, *The theory and practice of scintillation counting* (Pergamon Press, New York, 1964) p. 592.

5) E. L. Garwin, Y. Tomkiewicz and D. Trines, Nucl. Instr. and Meth. **107** (1973) 365.

6) G. Hass and R. Tousey, J. Opt. Soc. Am. **49** (1959) 593, and **50** (1960) 586.

7) G. Hass et al., Appl. Opt. **7** (1968) 1535; **8** (1969) 1183; **10** (1971) 540; **10** (1971) 958; **11** (1972) 1590; **11** (1972) 2245; R. P. Madden, *Physics of thin films* (G. Haas, ed.; Academic Press, New York, 1963).

8) G. L. Weissler, *Handbuch der Physik* XXI, p. 304.

9) G. W. C. Kaye and T. H. Laby, *Table of physical and chemical constants*, 14th ed. (1973) p. 93; and Harshaw Chemical Co., Brochure on optical crystals.

10) A. H. Laufer, J. A. Pirog and J. R. McNesby, J. Opt. Soc. Am. **55** (1965) 64.

11) R. Foord, R. Jones, C. J. Oliver and E. R. Pike, Appl. Opt. **8** (1968) 1975.

12) W. D. Gunter, Jr., E. F. Erickson and G. R. Grant, Appl. Opt. **4** (1965) 512.

13) B. E. Rambo, A. F. Avionics Laboratory Report ALTOR 64-19 (April 1964).

14) W. D. Gunter, Jr., G. R. Grant and G. A. Shaw, Appl. Opt. **9** (1970) 251.

15) M. Brunet, M. Cantin, C. Julliot and J. Vasseur, J. Phys. Appl. **24** (1963) 53A.